Revised Version

DESY 06-016
KIAS-P06005

DESY 06-016
KIAS–P06005
hep-ph/0602131

Neutralino Production and Decay at an e^+e^- Linear Collider with Transversely Polarized Beams

S.Y. Choi[1], M. Drees[2], and J. Song[3]

[1] *Deutsches Elektronen–Synchrotron DESY, 22603 Hamburg, Germany*
and
Department of Physics and RIPC, Chonbuk National University, Jeonju 561-756, Korea[*]

[2] *KIAS, School of Physics, Seoul 130–012, Korea*
and
Physikalisches Institut, Universität Bonn, Nussallee 12, D53115 Bonn, Germany[†]

[3] *Department of Physics, Konkuk University, Seoul 143–701, Korea*

Abstract

Once supersymmetric neutralinos $\tilde{\chi}^0$ are produced copiously at e^+e^- linear colliders, their characteristics can be measured with high precision. In particular, the fundamental parameters in the gaugino/higgsino sector of the minimal supersymmetric extension of the standard model (MSSM) can be analyzed. Here we focus on the determination of possible CP–odd phases of these parameters. To that end, we exploit the electron/positron beam polarization, including transverse polarization, as well as the spin/angular correlations of the neutralino production $e^+e^- \to \tilde{\chi}^0_i \tilde{\chi}^0_j$ and subsequent 2–body decays $\tilde{\chi}^0_i \to \tilde{\chi}^0_k h, \tilde{\chi}^0_k Z, \tilde{\ell}^\pm_R \ell^\mp$, using (partly) optimized CP–odd observables. If no final–state polarizations are measured, the Z and h modes are independent of the $\tilde{\chi}^0_i$ polarization, but CP–odd observables constructed from the leptonic decay mode can help in reconstructing the neutralino sector of the CP–noninvariant MSSM. In this situation, transverse beam polarization does not seem to be particularly useful in probing explicit CP violation in the neutralino sector of the MSSM. This can most easily be accomplished using longitudinal beam polarization.

[*]Permanent Address
[†]Permanent Address

1 Introduction

In the minimal supersymmetric standard model (MSSM) [1], the spin-1/2 partners of the neutral gauge bosons, $\tilde{B}$ and $\widetilde{W}_3$, and of the neutral Higgs bosons, $\tilde{H}_1^0$ and $\tilde{H}_2^0$, mix to form the neutralino mass eigenstates χ_i^0 (i=1,2,3,4). The corresponding mass matrix in the $(\tilde{B}, \widetilde{W}_3, \tilde{H}_1^0, \tilde{H}_2^0)$ basis

$$\mathcal{M} = \begin{pmatrix} M_1 & 0 & -m_Z c_\beta s_W & m_Z s_\beta s_W \\ 0 & M_2 & m_Z c_\beta c_W & -m_Z s_\beta c_W \\ -m_Z c_\beta s_W & m_Z c_\beta c_W & 0 & -\mu \\ m_Z s_\beta s_W & -m_Z s_\beta c_W & -\mu & 0 \end{pmatrix} \tag{1}$$

contains several fundamental supersymmetry parameters: the U(1) and SU(2) gaugino masses M_1 and M_2, the higgsino mass parameter μ, and the ratio $\tan\beta = v_2/v_1$ of the vacuum expectation values of the two neutral Higgs fields. Here, $s_\beta = \sin\beta$, $c_\beta = \cos\beta$ and s_W, c_W are the sine and cosine of the electroweak mixing angle θ_W.

In CP–noninvariant theories, the mass parameters $M_{1,2}$ and μ are complex. By re-parameterizing the fields, M_2 can be taken real and positive without loss of generality. Two remaining non–trivial phases are attributed to M_1 and μ:

$$M_1 = |M_1|\, \mathrm{e}^{i\Phi_1} \qquad \text{and} \qquad \mu = |\mu|\, \mathrm{e}^{i\Phi_\mu} \qquad (0 \le \Phi_1, \Phi_\mu < 2\pi)\,. \tag{2}$$

The existence of CP–violating phases in supersymmetric theories induces, in general, electric dipole moments (EDM) [2]. The current experimental bounds on the EDM's constrain the parameter space including many parameters outside the neutralino/chargino sector [3]. Detailed analyses of the electron EDM show [3, 4] that the phase Φ_μ must be quite small, unless selectrons are very heavy.* In contrast, large values of Φ_1 are allowed even for rather small selectron masses. The CP–violating phase Φ_1 can therefore play a significant role in the production and decay of neutralinos, which is most easily investigated at (linear) e^+e^- colliders [5, 6, 7, 4, 8].

Neutralinos are produced in e^+e^- collisions, either in diagonal or mixed pairs [9]. If the collider energy is high enough to produce all four neutralino states, the underlying SUSY parameters $\{|M_1|, \Phi_1, M_2, |\mu|, \Phi_\mu; \tan\beta\}$ can be extracted from the masses $m_{\tilde{\chi}_i^0}$ (i=1,2,3,4) and the cross sections [10, 11]. At the first stage of operations of a linear e^+e^- collider, however, only the lighter neutralinos may be accessible. If $\tilde{\chi}_1^0\tilde{\chi}_2^0$ is the only visible neutralino pair that is accessible, measuring their masses and (polarized) production cross sections may not suffice to determine the parameters of the neutralino mass matrix completely; the detailed analysis of $\tilde{\chi}_2^0$ decays will then be very useful. Moreover, even if sufficiently many different $\tilde{\chi}_i^0\tilde{\chi}_j^0$ states are accessible to determine all the parameters appearing in Eq. (1), analyses of neutralino decay will offer valuable redundancy. After

*Large values of Φ_μ can also be tolerated for moderate selectron masses if $\tan\beta$ is close to 1. However, this possibility is essentially excluded by Higgs boson searches at LEP.

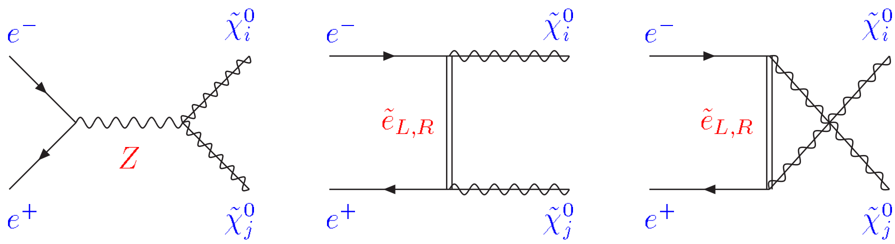

Figure 1: *Feynman diagrams for five mechanisms contributing to the production of diagonal and non–diagonal neutralino pairs in* e^+e^- *annihilation,* $e^+e^- \to \tilde\chi^0_i\tilde\chi^0_j$ $(i,j{=}1\text{–}4)$.

all, a theory can only be said to be tested successfully if experiments over–constrain its parameters.

In the present work we systematically investigate, both analytically and numerically, the usefulness of electron and positron beam polarization, including transverse polarization, for the analysis of neutralino production and decay at e^+e^- colliders. To this end, we exploit spin/angular correlations of the neutralino production $e^+e^- \to \tilde\chi^0_2\tilde\chi^0_1$ and subsequent two–body decays of $\tilde\chi^0_2 \to \tilde\chi^0_1 h, \tilde\chi^0_1 Z$, and $\tilde\chi^0_2 \to \tilde\ell^\pm\ell^\mp$ followed by $\tilde\ell^\pm \to \ell^\pm\tilde\chi^0_1$ for probing the CP properties of the neutralino sector in the MSSM. Due to the Majorana nature of neutralinos, the decay distributions of two–body decays $\tilde\chi^0_2 \to \tilde\chi^0_1 h, \tilde\chi^0_1 Z$ are independent of the $\tilde\chi^0_2$ polarization, unless the polarization of the Z boson is measured. These modes can still be used to probe a production–level CP–odd asymmetry, which however turns out to be small in the MSSM. The slepton mode $\tilde\chi^0_2 \to \tilde\ell^\pm_R\ell^\mp$ is an optimal polarization analyzer of the decaying neutralino. We can construct several CP–odd "decay" asymmetries that are sensitive to the $\tilde\chi^0_2$ polarization vector. Our main emphasis is on observables that *fully* reflect the non–trivial angular dependence of CP–odd terms, except for the angular dependence appearing in the propagators. Although they are not perfectly optimal, these CP–odd asymmetries have much higher statistical significance than the conventional ones, as demonstrated with numerical examples below.

The remainder of this article is organized as follows. Section 2 describes neutralino production, including the polarization of the neutralinos, for arbitrary beam polarization. Two–body decays of polarized neutralinos are discussed in Sec. 3. Section 4 deals with the reconstruction of $\tilde\chi^0_1\tilde\chi^0_2$ final states with invisible $\tilde\chi^0_1$. The formalism of "effective asymmetries" is described in Sec. 5, and numerical examples for these asymmetries are shown in Sec. 6. Finally, Section 7 contains a brief summary and some conclusions.

2 Neutralino production in e^+e^- collisions

The neutralino pair production processes in e^+e^- collisions

$$e^-(p,\sigma) + e^+(\bar p,\bar\sigma) \to \tilde\chi^0_i(p_i,\lambda_i) + \tilde\chi^0_j(p_j,\lambda_j) \qquad (\, i,j = 1,2,3,4) \tag{3}$$

are generated by the five mechanisms of the Feynman diagrams in Fig. 1, with s–channel Z exchange, or t– or u–channel $\tilde{e}_{L,R}$ exchange. Here σ, $\bar{\sigma}$, λ_i, and λ_j denote helicities. For the analytical calculation, we take a coordinate system where the production occurs in the (x, z) plane and the incident electron beam moves into $+z$ direction. The four–momenta appearing in Eq. (3) are then given by

$$
\begin{aligned}
p &= \frac{\sqrt{s}}{2}(1,\, 0,\, 0, \quad 1)\,, \\
\bar{p} &= \frac{\sqrt{s}}{2}(1,\, 0,\, 0, -1)\,, \\
p_i &= \frac{\sqrt{s}}{2}(e_i, \quad \lambda^{1/2}\sin\Theta,\, 0, \quad \lambda^{1/2}\cos\Theta)\,, \\
p_j &= \frac{\sqrt{s}}{2}(e_j, -\lambda^{1/2}\sin\Theta,\, 0, -\lambda^{1/2}\cos\Theta)\,,
\end{aligned}
\tag{4}
$$

where

$$
\begin{aligned}
&e_i = 1 + \mu_i^2 - \mu_j^2\,, \qquad e_j = 1 + \mu_j^2 - \mu_i^2\,, \\
&\mu_{i,j} = m_{\tilde{\chi}^0_{i,j}}/\sqrt{s}\,, \qquad \lambda = (1 - \mu_i^2 - \mu_j^2)^2 - 4\mu_i^2\mu_j^2\,.
\end{aligned}
\tag{5}
$$

The transition matrix element, after an appropriate Fierz transformation of the $\tilde{e}_{L,R}$ exchange amplitudes, can be expressed in terms of four generalized bilinear charges $Q_{\alpha\beta}$:

$$
T\left(e^+e^- \to \tilde{\chi}^0_i\tilde{\chi}^0_j\right) = \frac{e^2}{s}\, Q_{\alpha\beta}\left[\bar{v}(e^+)\gamma_\mu P_\alpha u(e^-)\right]\left[\bar{u}(\tilde{\chi}^0_i)\gamma^\mu P_\beta v(\tilde{\chi}^0_j)\right]\,. \tag{6}
$$

These generalized charges correspond to independent helicity amplitudes which describe the neutralino production processes for completely (longitudinally) polarized electrons and positrons, neglecting the electron mass as well as $\tilde{e}_L$–$\tilde{e}_R$ mixing.* They are defined in terms of the lepton and neutralino couplings as well as the propagators of the exchanged (s)particles [6, 11]:

$$
\begin{aligned}
Q_{LL} &= +\frac{D_Z}{s_W^2 c_W^2}\,(s_W^2 - \tfrac{1}{2})\mathcal{Z}_{ij} - D_{uL}\, g_{Lij}\,, \\
Q_{RL} &= +\frac{D_Z}{c_W^2}\,\mathcal{Z}_{ij} + D_{tR}\, g_{Rij}\,, \\
Q_{LR} &= -\frac{D_Z}{s_W^2 c_W^2}\,(s_W^2 - \tfrac{1}{2})\mathcal{Z}^*_{ij} + D_{tL}\, g^*_{Lij}\,, \\
Q_{RR} &= -\frac{D_Z}{c_W^2}\mathcal{Z}^*_{ij} - D_{uR}\, g^*_{Rij}\,.
\end{aligned}
\tag{7}
$$

*$\tilde{f}_L$–$\tilde{f}_R$ mixing is proportional to m_f unless one tolerates deeper minima of the scalar potential where charged sfermion fields obtain nonvanishing vacuum expectation values; although it can be enhanced at large $\tan\beta$ or for large trilinear A–parameters, selectron mixing is generally negligible for collider physics purposes.

The first index in $Q_{\alpha\beta}$ refers to the chirality of the $e^{\pm}$ current, the second index to the chirality of the $\tilde{\chi}^0$ current. The first term in each bilinear charge is generated by Z–exchange and the second term by selectron exchange; D_Z, $D_{tL,R}$ and $D_{uL,R}$ respectively denote the s–channel Z propagator and the t– and u–channel left/right–type selectron propagators:

$$
\begin{aligned}
D_Z &= \frac{s}{s - m_Z^2 + i m_Z \Gamma_Z}\,, \\
D_{tL,R} &= \frac{s}{t - m_{\tilde{e}_{L,R}}^2} \qquad \text{and} \qquad t \to u\,,
\end{aligned}
\tag{8}
$$

with $s = (p + \bar{p})^2$, $t = (p - p_i)^2$ and $u = (p - p_j)^2$. The matrices $\mathcal{Z}_{ij}$, g_{Lij} and g_{Rij} can be computed from the matrix N diagonalizing the neutralino mass matrix [1]

$$
\begin{aligned}
\mathcal{Z}_{ij} &= (N_{i3} N_{j3}^* - N_{i4} N_{j4}^*)/2\,, \\
g_{Lij} &= (N_{i2} c_W + N_{i1} s_W)(N_{j2}^* c_W + N_{j1}^* s_W)/4 s_W^2 c_W^2\,, \\
g_{Rij} &= N_{i1} N_{j1}^*/c_W^2\,.
\end{aligned}
\tag{9}
$$

They satisfy the hermiticity relations of

$$
\mathcal{Z}_{ij} = \mathcal{Z}_{ji}^*\,, \qquad g_{Lij} = g_{Lji}^*\,, \qquad g_{Rij} = g_{Rji}^*\,. \tag{10}
$$

If the decay width Γ_Z is neglected in the Z boson propagator D_Z, the bilinear charges $Q_{\alpha\beta}$ satisfy similar relations, $Q_{\alpha\beta}(\tilde{\chi}_i^0, \tilde{\chi}_j^0, t, u) = Q_{\alpha\beta}^*(\tilde{\chi}_j^0, \tilde{\chi}_i^0, u, t)$. These relations are very useful in classifying CP–even and CP–odd observables.

2.1 Production helicity amplitudes

With the $e^{\pm}$ mass neglected, the matrix element in Eq. (6) is nonzero only if the electron helicity is opposite to the positron helicity. We write the helicity amplitudes as

$$
T(\sigma, \bar{\sigma}, \lambda_i, \lambda_j) = T(\sigma, -\sigma, \lambda_i, \lambda_j)\; \delta_{\bar{\sigma}, -\sigma} \equiv 2\pi\alpha\, \langle \sigma; \lambda_i\, \lambda_j \rangle\; \delta_{\bar{\sigma}, -\sigma}\,, \tag{11}
$$

where $\sigma, \lambda_i, \lambda_j = \pm$. Explicit expressions for these helicity amplitudes are [6]:

$$
\begin{aligned}
\langle +; ++ \rangle &= -\left[Q_{RR}\sqrt{\eta_{i+}\eta_{j-}} + Q_{RL}\sqrt{\eta_{i-}\eta_{j+}}\right] \sin\Theta\,, \\
\langle +; +- \rangle &= -\left[Q_{RR}\sqrt{\eta_{i+}\eta_{j+}} + Q_{RL}\sqrt{\eta_{i-}\eta_{j-}}\right] (1 + \cos\Theta)\,, \\
\langle +; -+ \rangle &= +\left[Q_{RR}\sqrt{\eta_{i-}\eta_{j-}} + Q_{RL}\sqrt{\eta_{i+}\eta_{j+}}\right] (1 - \cos\Theta)\,, \\
\langle +; -- \rangle &= +\left[Q_{RR}\sqrt{\eta_{i-}\eta_{j+}} + Q_{RL}\sqrt{\eta_{i+}\eta_{j-}}\right] \sin\Theta\,, \\
\langle -; ++ \rangle &= -\left[Q_{LL}\sqrt{\eta_{i-}\eta_{j+}} + Q_{LR}\sqrt{\eta_{i+}\eta_{j-}}\right] \sin\Theta\,, \\
\langle -; +- \rangle &= +\left[Q_{LL}\sqrt{\eta_{i-}\eta_{j-}} + Q_{LR}\sqrt{\eta_{i+}\eta_{j+}}\right] (1 - \cos\Theta)\,, \\
\langle -; -+ \rangle &= -\left[Q_{LL}\sqrt{\eta_{i+}\eta_{j+}} + Q_{LR}\sqrt{\eta_{i-}\eta_{j-}}\right] (1 + \cos\Theta)\,, \\
\langle -; -- \rangle &= +\left[Q_{LL}\sqrt{\eta_{i+}\eta_{j-}} + Q_{LR}\sqrt{\eta_{i-}\eta_{j+}}\right] \sin\Theta\,,
\end{aligned}
\tag{12}
$$

where $\eta_{i\pm} = e_i \pm \lambda^{1/2}$ and $\eta_{j\pm} = e_j \pm \lambda^{1/2}$. In the high energy asymptotic limit, η_{i+} and η_{i-} approach 1 and 0, respectively; only the helicity amplitudes with opposite $\tilde{\chi}_i^0$ and $\tilde{\chi}_j^0$ helicities survive.

2.2 Production cross sections

We analyze neutralino production for general $e^{\pm}$ polarization states. With the scattering plane fixed as the (x, z) plane, the azimuthal scattering angle appears in the description of the $e^{\pm}$ polarization vectors:

$$\overrightarrow{P}_{e^-} = (P_T\cos\Phi, -P_T\sin\Phi, P_L), \quad \overrightarrow{P}_{e^+} = (\overline{P}_T\cos(\eta-\Phi), \overline{P}_T\sin(\eta-\Phi), -\overline{P}_L)\,, \tag{13}$$

where η is the relative angle between the transverse components of two polarization vectors. The density matrices ρ $(\overline{\rho})$ of the electron (positron) in the $\{+,-\}$ helicity basis are [13]

$$\rho = \frac{1}{2}\begin{pmatrix} 1+P_L & P_T e^{i\Phi} \\ P_T e^{-i\Phi} & 1-P_L \end{pmatrix}, \qquad \overline{\rho} = \frac{1}{2}\begin{pmatrix} 1+\overline{P}_L & -\overline{P}_T e^{-i(\eta-\Phi)} \\ -\overline{P}_T e^{i(\eta-\Phi)} & 1-\overline{P}_L \end{pmatrix}. \tag{14}$$

The polarized differential cross section is given by

$$\frac{d\sigma}{d\Omega} = \frac{\lambda^{1/2}}{64\pi^2 s}\overline{|T|^2}\,, \tag{15}$$

where

$$\overline{|T|^2} = \sum_{\sigma,\bar\sigma,\lambda_i,\lambda_j} T(\sigma,\bar\sigma,\lambda_i,\lambda_j)T^*(\sigma',\bar\sigma',\lambda_i,\lambda_j)\,\rho_{\sigma\sigma'}\,\overline{\rho}_{\bar\sigma'\bar\sigma}\,. \tag{16}$$

Note that the order of indices of $\overline{\rho}_{\bar\sigma'\bar\sigma}$ is opposite of that of $\rho_{\sigma\sigma'}$ due to the difference between the particle and the antiparticle. Inserting Eqs. (12) and (14) into Eq. (16) yields

$$\begin{aligned}\frac{d\sigma}{d\Omega}\{ij\} = \frac{\alpha^2}{4s}\,\lambda^{1/2}\Big[&(1-P_L\bar P_L)\,\Sigma^{ij}_{UU} + (P_L-\bar P_L)\,\Sigma^{ij}_{UL} \\ &+ P_T\bar P_T\cos(2\Phi-\eta)\,\Sigma^{ij}_{UT} + P_T\bar P_T\sin(2\Phi-\eta)\,\Sigma^{ij}_{UN}\Big]\,,\end{aligned} \tag{17}$$

where

$$\begin{aligned}\Sigma^{ij}_{UU} &= \left[1-(\mu_i^2-\mu_j^2)^2+\lambda\cos^2\Theta\right]Q_1 + 4\mu_i\mu_j Q_2 + 2\lambda^{1/2}Q_3\cos\Theta, \\ \Sigma^{ij}_{UL} &= \left[1-(\mu_i^2-\mu_j^2)^2+\lambda\cos^2\Theta\right]Q_1' + 4\mu_i\mu_j Q_2' + 2\lambda^{1/2}Q_3'\cos\Theta, \\ \Sigma^{ij}_{UT} &= \lambda\,Q_5\sin^2\Theta, \\ \Sigma^{ij}_{UN} &= -\lambda\,Q_6'\sin^2\Theta\,.\end{aligned} \tag{18}$$

Expressions for all relevant quartic charges $Q_i^{(\prime)}$ in terms of bilinear charges $Q_{\alpha\beta}$ are given in Table 1, which also lists the transformation properties under P and CP. Non–zero transverse $e^{\pm}$ beam polarization allows to probe four new quartic charges, Q_5, Q_6, Q_5', and Q_6'.

Table 1: *The independent quartic charges describing* $e^+e^- \to \tilde{\chi}^0_i \tilde{\chi}^0_j$.

P	CP	Quartic charges
even	even	$Q_1 = \frac{1}{4}\left[\lvert Q_{RR}\rvert^2 + \lvert Q_{LL}\rvert^2 + \lvert Q_{RL}\rvert^2 + \lvert Q_{LR}\rvert^2\right]$
		$Q_2 = \frac{1}{2}\Re\mathrm{e}\left[Q_{RR}Q^*_{RL} + Q_{LL}Q^*_{LR}\right]$
		$Q_3 = \frac{1}{4}\left[\lvert Q_{RR}\rvert^2 + \lvert Q_{LL}\rvert^2 - \lvert Q_{RL}\rvert^2 - \lvert Q_{LR}\rvert^2\right]$
		$Q_5 = \frac{1}{2}\Re\mathrm{e}\left[Q_{RR}Q^*_{LR} + Q_{LL}Q^*_{RL}\right]$
	odd	$Q_4 = \frac{1}{2}\Im\mathrm{m}\left[Q_{RR}Q^*_{RL} + Q_{LL}Q^*_{LR}\right]$
		$Q_6 = \frac{1}{2}\Im\mathrm{m}\left[Q_{RR}Q^*_{LR} + Q_{LL}Q^*_{RL}\right]$
odd	even	$Q'_1 = \frac{1}{4}\left[\lvert Q_{RR}\rvert^2 + \lvert Q_{RL}\rvert^2 - \lvert Q_{LL}\rvert^2 - \lvert Q_{LR}\rvert^2\right]$
		$Q'_2 = \frac{1}{2}\Re\mathrm{e}\left[Q_{RR}Q^*_{RL} - Q_{LL}Q^*_{LR}\right]$
		$Q'_3 = \frac{1}{4}\left[\lvert Q_{RR}\rvert^2 + \lvert Q_{LR}\rvert^2 - \lvert Q_{LL}\rvert^2 - \lvert Q_{RL}\rvert^2\right]$
		$Q'_5 = \frac{1}{2}\Re\mathrm{e}\left[Q_{RR}Q^*_{LR} - Q_{LL}Q^*_{RL}\right]$
	odd	$Q'_4 = \frac{1}{2}\Im\mathrm{m}\left[Q_{RR}Q^*_{RL} - Q_{LL}Q^*_{LR}\right]$
		$Q'_6 = \frac{1}{2}\Im\mathrm{m}\left[Q_{RR}Q^*_{LR} - Q_{LL}Q^*_{RL}\right]$

2.3 Neutralino polarization vector

The polarization vector $\vec{\mathcal{P}}^i = (\mathcal{P}^i_T, \mathcal{P}^i_N, \mathcal{P}^i_L)$ of the neutralino $\tilde{\chi}^0_i$ is defined in its rest frame. The longitudinal component $\mathcal{P}^i_L$ is parallel to the $\tilde{\chi}^0_i$ flight direction in the c.m. frame, $\mathcal{P}^i_T$ is in the production plane, and $\mathcal{P}^i_N$ is normal to the production plane. In order to extract the vector $\vec{\mathcal{P}}^i$, we first define the polarization density matrix for the out–going neutralino $\tilde{\chi}^0_i$:

$$\rho^i_{\lambda_i\lambda'_i} = \frac{\sum_{\sigma,\lambda_j}\langle\sigma;\lambda_i\lambda_j\rangle\langle\sigma;\lambda'_i\lambda_j\rangle^*}{\sum_{\sigma,\lambda_i,\lambda_j}\langle\sigma;\lambda_i\lambda_j\rangle\langle\sigma;\lambda_i\lambda_j\rangle^*}\,. \tag{19}$$

Explicit expressions for the helicity amplitudes $\langle\sigma;\lambda_i\lambda_j\rangle$ are given in Eq. (12). The polarization vector of the neutralino $\tilde{\chi}^0_i$ is then given by

$$\vec{\mathcal{P}}^i = \mathrm{Tr}(\vec{\sigma}\rho^i) = \frac{1}{\Delta^{ij}_U}\left(\Delta^{ij}_T, \Delta^{ij}_N, \Delta^{ij}_L\right)\,. \tag{20}$$

We can decompose the three polarization components as well as the unpolarized part according to combinations of $e^\pm$ polarizations:

$$\Delta^{ij}_U = (1 - P_L\overline{P}_L)\Sigma^{ij}_{UU} + (P_L - \overline{P}_L)\Sigma^{ij}_{UL} + P_T\overline{P}_T\{\Sigma^{ij}_{UT}c_{(2\Phi-\eta)} + \Sigma^{ij}_{UN}s_{(2\Phi-\eta)}\}\,,$$

$$
\begin{aligned}
\Delta^{ij}_L &= (1-P_L\overline{P}_L)\Sigma^{ij}_{LU} + (P_L-\overline{P}_L)\Sigma^{ij}_{LL} + P_T\overline{P}_T\{\Sigma^{ij}_{LT}c_{(2\Phi-\eta)} + \Sigma^{ij}_{LN}s_{(2\Phi-\eta)}\}\,,\\
\Delta^{ij}_T &= (1-P_L\overline{P}_L)\Sigma^{ij}_{TU} + (P_L-\overline{P}_L)\Sigma^{ij}_{TL} + P_T\overline{P}_T\{\Sigma^{ij}_{TT}c_{(2\Phi-\eta)} + \Sigma^{ij}_{TN}s_{(2\Phi-\eta)}\}\,,\\
\Delta^{ij}_N &= (1-P_L\overline{P}_L)\Sigma^{ij}_{NU} + (P_L-\overline{P}_L)\Sigma^{ij}_{NL} + P_T\overline{P}_T\{\Sigma^{ij}_{NT}c_{(2\Phi-\eta)} + \Sigma^{ij}_{NN}s_{(2\Phi-\eta)}\}\,, \qquad (21)
\end{aligned}
$$

where $c_{(2\Phi-\eta)} = \cos(2\Phi-\eta)$, $s_{(2\Phi-\eta)} = \sin(2\Phi-\eta)$, and the Σ_{UB} ($B = U,\, L,\, T,\, N$) are in Eq. (18). The Σ_{BU}, which survive even without beam polarization, are given by

$$
\begin{aligned}
\Sigma^{ij}_{LU} &= 2(1-\mu_i^2-\mu_j^2)\,\cos\Theta\, Q'_1 + 4\mu_i\mu_j\,\cos\Theta\, Q'_2 + \lambda^{1/2}\{1+\cos^2\Theta - \sin^2\Theta(\mu_i^2-\mu_j^2)\}\, Q'_3\,,\\
\Sigma^{ij}_{TU} &= -2\sin\Theta\left[\{(1-\mu_i^2+\mu_j^2)\,Q'_1 + \lambda^{1/2}\cos\Theta\, Q'_3\}\mu_i + (1+\mu_i^2-\mu_j^2)\mu_j\, Q'_2\right]\,,\\
\Sigma^{ij}_{NU} &= 2\lambda^{1/2}\mu_j\,\sin\Theta\, Q_4\,. \qquad (22)
\end{aligned}
$$

The remaining Σ_{AB}, which contribute only with non–trivial $e^\pm$ polarization, are

$$
\begin{aligned}
\Sigma^{ij}_{LL} &= [\lambda+1-(\mu_i^2-\mu_j^2)^2]\,\cos\Theta\, Q_1 + 4\mu_i\mu_j\,\cos\Theta\, Q_2\\
&\qquad +\lambda^{1/2}[1+\cos^2\Theta - \sin^2\Theta\,(\mu_i^2-\mu_j^2)]\, Q_3\,,\\
\Sigma^{ij}_{LT} &= \lambda^{1/2}(1+\mu_i^2-\mu_j^2)\sin^2\Theta\, Q'_5\,,\\
\Sigma^{ij}_{LN} &= -\lambda^{1/2}(1+\mu_i^2-\mu_j^2)\sin^2\Theta\, Q_6\,,\\
\Sigma^{ij}_{TL} &= -2\sin\Theta\left\{[(1-\mu_i^2+\mu_j^2)\,Q_1 + \lambda^{1/2}\cos\Theta\, Q_3]\mu_i + (1+\mu_i^2-\mu_j^2)\mu_j\, Q_2\right\}\,,\\
\Sigma^{ij}_{TT} &= \lambda^{1/2}\mu_i\sin 2\Theta\, Q'_5\,,\\
\Sigma^{ij}_{TN} &= -\lambda^{1/2}\mu_i\sin 2\Theta\, Q_6\,,\\
\Sigma^{ij}_{NL} &= 2\lambda^{1/2}\mu_j\,\sin\Theta\, Q'_4\,,\\
\Sigma^{ij}_{NT} &= -2\lambda^{1/2}\mu_i\,\sin\Theta\, Q_6\,,\\
\Sigma^{ij}_{NN} &= -2\lambda^{1/2}\mu_i\,\sin\Theta\, Q'_5\,. \qquad (23)
\end{aligned}
$$

The P and CP properties of all these quantities are identical to those of the quartic charges in Table 1. In particular, the five quantities $\Sigma_{UN}, \Sigma_{LN}, \Sigma_{TN}, \Sigma_{NU}$ and Σ_{NL} are CP–odd.

Brief comments on the reference frame are in order here. In the coordinate system which we have employed so far, the scattering plane is fixed, while the direction of $e^\pm$ transverse polarization vectors differs from event to event. For a real experiment, fixed $e^\pm$ polarization vectors should be more convenient. We define the transverse part of $\vec{P}_{e^-}$ as $+x$ direction; the x and y components of the outgoing neutralino four–momentum p_i are then proportional to $\cos\Phi$ and $\sin\Phi$, respectively. In this coordinate system the scattering plane changes from event to event. Since only the relative angles between the $e^\pm$ polarization vectors and the scattering plane are relevant, the final results in Eqs. (17) and (21) are still valid. In this new coordinate frame, the $\tilde{\chi}^0_i$ polarization vector can be explicitly written as

$$
\vec{\mathcal{P}}^i = \mathcal{P}^i_T\vec{e}_T + \mathcal{P}^i_N\vec{e}_N + \mathcal{P}^i_L\vec{e}_L\,, \qquad (24)
$$

where the following three unit vectors form a co–moving orthonormal basis of the three–dimensional space:

$$
\vec{e}_T \;=\; (\cos\Phi\cos\Theta,\, \sin\Phi\cos\Theta,\, -\sin\Theta)\,,
$$

$$
\begin{aligned}
\vec{e}_N &= (-\sin\Phi,\, \cos\Phi,\, 0)\,, \\
\vec{e}_L &= (\cos\Phi\sin\Theta,\, \sin\Phi\sin\Theta,\, \cos\Theta)\,.
\end{aligned} \tag{25}
$$

Probing CP violation in the MSSM neutralino sector involves the four quartic charges Q_4, Q_4', Q_6 and Q_6' for $i \neq j$. Their characteristic features can be analytically understood from their explicit expressions in terms of the neutralino mixing matrix N. With Γ_Z neglected in the high energy limit, they are

$$
\begin{aligned}
Q_4^{(\prime)} &= \frac{1}{2c_W^4 s_W^4}\left[s_W^4 \mp (s_W^2-1/2)^2\right] D_Z^2 \Im\mathrm{m}(\mathcal{Z}_{ij}^2) \\
&\quad + \frac{D_Z}{2c_W^2}\left[(D_{tR}+D_{uR})\Im\mathrm{m}(\mathcal{Z}_{ij} g_{Rij}) \pm \frac{s_W^2-1/2}{s_W^2}(D_{tL}+D_{UL})\Im\mathrm{m}(\mathcal{Z}_{ij} g_{Lij})\right] \\
&\quad + \frac{1}{2} D_{uR} D_{tR} \Im\mathrm{m}(g_{Rij}^2) \mp \frac{1}{2} D_{uL} D_{tL} \Im\mathrm{m}(g_{Lij}^2)\,, \\
Q_6^{(\prime)} &= \frac{1}{2c_W^2} D_Z (D_{tL} \pm D_{uL}) \Im\mathrm{m}(\mathcal{Z}_{ij} g_{Lij}^*) + \frac{s_W^2-1/2}{2s_W^2 c_W^2} D_Z (D_{uR} \pm D_{tR}) \Im\mathrm{m}(\mathcal{Z}_{ij} g_{Rij}^*) \\
&\quad + \frac{1}{2}(D_{uR} D_{tL} \pm D_{tR} D_{uL}) \Im\mathrm{m}(g_{Lij} g_{Rij}^*)\,,
\end{aligned} \tag{26}
$$

where the explicit form of $\mathcal{Z}_{ij}$, g_{Lij} and g_{Rij} are listed in Eq. (9). From the propagator combinations, we see that the quartic charge Q_6' is forward–backward asymmetric with respect to the scattering angle Θ while the other three quartic charges, $Q_4^{(\prime)}$ and Q_6, are forward–backward symmetric.

The relative sizes of the four CP–violating quartic charges indicate which observables should be promising to investigate experimentally. Let us first consider the generic case of small gaugino–higgsino mixing (with substantial CP phase Φ_1). Small mixing is generally obtained if the entries in the off–diagonal 2×2 blocks in the neutralino mass matrix are smaller than those in the diagonal blocks, allowing an expansion in powers of m_Z. Analytic expressions for N using this expansion, given in Ref. [4], help to estimate the sizes of the Q $Q_{4,6}^{(\prime)}$. In particular, the last term contributing to $Q_4^{(\prime)}$ in Eq. (26), which is proportional to $\sin\Phi_1$, is not suppressed by small mixing angles: Q_4 and Q_4' survive even without any gaugino–higgsino mixing. In contrast Q_6 and Q_6' only start at $O(m_Z^2)$. This is related to the observation that, in the notation of Ref. [11], $Q_6^{(\prime)}$ probe Dirac–type phases, which vanish in the absence of nontrivial mixing between neutralino current eigenstates, whereas $Q_4^{(\prime)}$ probe Majorana–type phases, which survive in this limit. In the generic case of small gaugino–higgsino mixing, therefore, the size of $Q_4^{(\prime)}$ is much larger than that of $Q_6^{(\prime)}$. In the case of strong gaugino–higgsino mixing, however, $Q_6^{(\prime)}$, which can only be probed with transversely polarized beams, could exceed Q_4 and/or Q_4'.

3 Two–body neutralino decays

The decay patterns of heavy neutralinos ($\tilde{\chi}^0_{i>1}$) depend on their masses and the masses and couplings of other sparticles and Higgs bosons. In this article we focus on the two–body decays of neutralinos. It is possible that the kinematics prohibits some two–body tree–level decays. However, a sufficiently heavy neutralino can decay via tree–level two–body channels containing a Z or a Higgs boson and a lighter neutralino [14], and/or into a sfermion–matter fermion pair.

Of particular interest in the present work are the following two–body decay modes:

$$\tilde{\chi}^0_i \to \tilde{\chi}^0_k\, Z, \qquad \tilde{\chi}^0_i \to \tilde{\chi}^0_k\, h \quad \text{and} \quad \tilde{\chi}^0_i \to \tilde{\ell}^\pm_R \ell^\mp\,, \tag{27}$$

with $\ell = e$ or μ. If any of these processes is kinematically allowed, it will dominate any tree–level three–body decay.

The relevant couplings are

$$\begin{aligned}
&\langle\, \ell^-_L \,|\, \tilde{\ell}^-_R \,|\tilde{\chi}^0_i\,\rangle = +\langle\, \ell^+_L \,|\, \tilde{\ell}^+_R \,|\tilde{\chi}^0_i\,\rangle^* = -\sqrt{2} g t_W\, N^*_{i1}, \qquad \langle \ell^\pm_R | \tilde{\ell}^\pm_R | \tilde{\chi}^0_i \rangle = 0\,, \\
&\langle \tilde{\chi}^0_{kR} | Z | \tilde{\chi}^0_{iR} \rangle = -\langle \tilde{\chi}^0_{kL} | Z | \tilde{\chi}^0_{iL} \rangle^* = +\frac{g}{2c_W}\left[N_{i3} N^*_{k3} - N_{i4} N^*_{k4} \right]\,, \\
&\langle \tilde{\chi}^0_{kL} | h | \tilde{\chi}^0_{iR} \rangle = +\langle \tilde{\chi}^0_{kR} | h | \tilde{\chi}^0_{iL} \rangle^* = \frac{g}{2}\left[(N_{k2} - t_W N_{k1})(s_\alpha N_{i3} + c_\alpha N_{i4}) + (i \leftrightarrow k) \right]\,,
\end{aligned} \tag{28}$$

where $s_\alpha = \cos\alpha$, $c_\alpha = \sin\alpha$, and α being the mixing angle between the two CP–even Higgs states in the MSSM [1]. Note that the Z coupling is proportional to the higgsino components of both participating neutralinos, whereas the Higgs coupling requires a higgsino component of one neutralino and a gaugino component of the other.* Since the lighter neutralino states $\tilde{\chi}^0_{1,2}$ are often gaugino–like, this pattern of couplings implies that $\tilde{\chi}^0_i \to \tilde{\chi}^0_1 h$ decays will often dominate over the (kinematically preferred) $\tilde{\chi}^0_i \to \tilde{\chi}^0_1 Z$ decays. However, the $\tilde{\chi}^0_i \to \tilde{\ell}^\pm_R \ell^\mp$ decays only depend on the gaugino components of the decaying neutralino. If kinematically accessible, they can have the largest branching ratios.

Note also that the Majorana nature of neutralinos relates the left– and right–handed couplings of the Z and h boson to a neutralino pair; they are complex conjugate to each other, having an identical absolute magnitude. These relations lead to a characteristic property of the corresponding two–body decays, $\tilde{\chi}^0_i \to \tilde{\chi}^0_k Z$ and $\tilde{\chi}^0_i \to \tilde{\chi}^0_k h$: *the decay distributions are independent of the polarization of the decaying neutralino $\tilde{\chi}^0_i$, unless the polarization of the Z boson or $\tilde{\chi}^0_k$ is measured.* In contrast, the slepton mode in Eq. (27) can be exploited as optimal polarization analyzer of the decaying neutralino, if the small lepton mass is ignored; as noted earlier, this implies that $\tilde{\ell}_L$–$\tilde{\ell}_R$ mixing is ignored as well.†

*If $\delta m_{\tilde{\chi}} \equiv m_{\tilde{\chi}^0_2} - m_{\tilde{\chi}^0_1} \gg m_Z$, the decay into longitudinally polarized Z bosons gets enhanced by a factor $(\delta m_{\tilde{\chi}}/m_Z)^2$. If $\delta m_{\tilde{\chi}} \sim \mathcal{O}(m_Z)$, three–body decays $\tilde{\chi}^0_2 \to \tilde{\chi}^0_1 f\bar{f}$ may dominate over $\tilde{\chi}^0_2 \to \tilde{\chi}^0_1 Z$ decays if $|\mu| \gg m_{\tilde{f}}$; this does not happen in models where the entire sparticle spectrum is described by a small number of parameters.

†$\tilde{\chi}_i \to \tilde{\tau}^\pm_1 \tau^\mp$ decays, where $\tilde{\tau}_L$–$\tilde{\tau}_R$ mixing can be important, have been analyzed in Refs. [7].

Furthermore, the decay distributions are completely determined by the relevant particle masses, as well as by the $\tilde{\chi}_i^0$ polarization vector (in case of $\tilde{\chi}_i^0 \to \tilde{\ell}_R^{\pm}\ell^{\mp}$ decay). More explicitly, the angular distribution in the rest frame of the decaying neutralino $\tilde{\chi}_i^0$ is

$$\frac{1}{\Gamma_X}\frac{d\Gamma_X}{d\Omega^*} = \frac{1}{4\pi}\left(1 \pm \xi_X \vec{\mathcal{P}}^i \cdot \hat{k}_1^*\right) , \tag{29}$$

where $\xi_{Z,h} = 0$ for the Z and h decay modes, and $\xi_{l^\pm} = \mp 1$ for $\tilde{\chi}_i^0 \to \tilde{\ell}_R^{\pm}\ell^{\mp}$ with $\hat{k}_1^*$ being the unit vector in $\ell^{\mp}$ direction. The former two decay modes can probe only "production" asymmetries, whereas the (s)leptonic decay mode can probe "decay" asymmetries also, which are sensitive to the $\tilde{\chi}_i^0$ polarization.

4 Event reconstruction

We focus on $e^+e^- \to \tilde{\chi}_2^0\tilde{\chi}_1^0$ production, and assume $\tilde{\chi}_1^0$ to be stable (or possibly to decay invisibly). The only visible final state particles therefore result from $\tilde{\chi}_2^0$ decay, which simplifies the analysis. Moreover, this is the kinematically most accessible neutralino pair production with visible final state; indeed, it is often the first sparticle production channel accessible at e^+e^- colliders [15].

An important difference between $\tilde{\chi}_2^0 \to \tilde{\chi}_1^0(h, Z)$ and $\tilde{\chi}_2^0 \to \tilde{\ell}_R^{\pm}\ell^{\mp} \to \tilde{\chi}_1^0\ell^+\ell^-$ is the degree of event reconstruction. The latter decay chain allows complete event reconstruction (with an, at least, two–fold ambiguity), whereas the former does not. This can be seen by counting unknowns. The $\tilde{\chi}_1^0\tilde{\chi}_1^0(h, Z)$ final states contain six unknown components of $\tilde{\chi}_1^0$ momenta (we are assuming that the masses of all produced particles have already been determined [10], so that the energies can be computed from three–momenta); this has to be compared with four constraints from energy–momentum conservation, and a single mass constraint, $(p_{\tilde{\chi}_1^0} + p_{(h,Z)})^2 = m^2_{\tilde{\chi}_2^0}$. One quantity remains undetermined.

In contrast, $\tilde{\chi}_1^0\tilde{\chi}_1^0\ell^+\ell^-$ final states produced from an on–shell $\tilde{\ell}_R^{\pm}$ have two invariant mass constraints. With an equal number of constraints and unknowns, the event can be reconstructed [8]. An explicit reconstruction may proceed as follows. Let k_1 and k_2 be the four–momenta of the two charged leptons in the final state, and p_1 and q the four–momenta of the two neutralinos; here k_2 and q originate from $\tilde{\ell}_R$ decay. Note that the energy p_1^0 is fixed from two–body kinematics, see Eq. (4). Then q^0 is determined from energy conservation, once the lepton energies are measured. The invariant mass constraint $(k_2 + q)^2 = m^2_{\tilde{\ell}_R}$ can fix the scalar product $\vec{k}_2 \cdot \vec{q}$. The second mass constraint $(k_1 + k_2 + q)^2 = m^2_{\tilde{\chi}_2^0}$ is used for $\vec{k}_1 \cdot \vec{q}$. When writing the unknown three–momentum $\vec{q}$ as $\vec{q} = a\vec{k}_1 + b\vec{k}_2 + c(\vec{k}_1 \times \vec{k}_2)$, the two coefficients a and b can be computed from the two scalar products $\vec{k}_2 \cdot \vec{q}$ and $\vec{k}_1 \cdot \vec{q}$ determined above; note that the term proportional to c drops out here. The last coefficient c can be computed from the known energy q^0 with two–fold ambiguity.

Once $\vec{q}$ is known, $\vec{p}_1$ follows immediately from momentum conservation. We can read off the production angles Θ and Φ. This also allows to compute the $\tilde{\chi}_2^0$ three–momentum $\vec{p}_2 = \vec{k}_1 + \vec{k}_2 + \vec{q} = -\vec{p}_1$ (in the c.m. frame). With the known $\tilde{\chi}_2^0$ energy, we boost into the $\tilde{\chi}_2^0$ rest frame, and read off the $\tilde{\chi}_2^0$ decay angles Θ^* and Φ^*; recall that there is a non–trivial dependence on these decay angles via Eq. (29).

So far we have assumed that we know which of the two charged leptons in the final state originates from the $\tilde{\chi}_2^0$ decay, and which one from $\tilde{\ell}_R$ decay. Since, owing to its Majorana nature, $\tilde{\chi}_2^0$ will decay into both $\tilde{\ell}_R^+\ell^-$ and $\tilde{\ell}_R^-\ell^+$ final states with equal branching ratios, the charge of the leptons does not help this discrimination of the origin of two charged leptons. A unique assignment is nevertheless possible if the two mass differences $\delta_{2R} \equiv m_{\tilde{\chi}_2^0} - m_{\tilde{\ell}_R}$ and $\delta_{R1} \equiv m_{\tilde{\ell}_R} - m_{\tilde{\chi}_1^0}$ are very different from each other: if $\delta_{2R} \gg \delta_{R1}$, the more energetic (harder) lepton will originate from the first step of $\tilde{\chi}_2^0$ decay, and the less energetic (softer) lepton comes from $\tilde{\ell}_R$ decay; if $\delta_{2R} \ll \delta_{R1}$ the opposite assignment holds. However, if $\delta_{2R} \simeq \delta_{R1}$, both assignments often lead to physical solutions if the procedure for event reconstruction outlined above is applied. In this unfavorable situation there is a four–fold ambiguity in the event reconstruction.

Finally, we note that background events can be also reconstructed, in some cases again with two–fold ambiguity. The main backgrounds to $\tilde{\chi}_2^0 \to \tilde{\chi}_1^0(Z,h)$ decays are $e^+e^- \to ZZ$, Zh production with one Z decaying invisibly. The $e^+e^- \to ZZ(\to \nu\bar{\nu}\ell^+\ell^-)$, $W^+W^-(\to \ell^+\nu_\ell\ell^-\bar{\nu}_\ell)$, $\tilde{\ell}^+\tilde{\ell}^-(\to \ell^+\ell^-\tilde{\chi}_1^0\tilde{\chi}_1^0)$ are the main backgrounds to $\tilde{\chi}_1^0\tilde{\chi}_2^0 \to \ell^+\ell^-\tilde{\chi}_1^0\tilde{\chi}_1^0$ production.* We can obtain a pure sample of signal events by discarding all events that can be reconstructed as one of the background processes. This ignores the effects of measurement errors, beam energy spread (partly due to bremsstrahlung), as well as initial state radiation, but should nevertheless give a reasonable indication of the effects of cuts that have to be imposed to isolate the signal.

5 Effective asymmetries

We are interested in constructing CP–odd observables. Schematically, they are written as

$$F = \int d\Omega \frac{d\sigma}{d\Omega} f(\Omega) \times \mathcal{L}\,, \tag{30}$$

where $d\sigma/d\Omega$ is the differential cross section, $\mathcal{L} = \int L\, dt$ is the total integrated luminosity, and $f(\Omega)$ is a dimensionless function of phase space observables. Introducing the luminosity in Eq. (30) simplifies the statistical analysis as presented below.

Simple asymmetries are constructed from the choice $f = \pm 1$, where the phase space region giving $f = +1$ is the CP–conjugate of that giving $f = -1$ [5, 8]. While very straightforward, this choice usually does not yield the highest statistical significance. We

*Note that we include supersymmetric slepton production as background, since it does not contribute to the CP–odd asymmetries we wish to analyze here.

decompose the differential cross section into CP–even and CP–odd terms:

$$\frac{d\sigma}{d\Omega} = \sum_i e_i f_i^{(e)}(\Omega) + \sum_j o_j f_j^{(o)}(\Omega)\,, \tag{31}$$

where the e_i and o_j are constant coefficients (products of couplings and possibly masses) while the $f^{(e)}$ and $f^{(o)}$ are CP–even and CP–odd functions, respectively, of phase space variables. The optimal variable to extract the coefficient o_j is then proportional to $f_j^{(o)}$ [16].

In our case this would lead to very complicated observables, due to the non–trivial angular dependence of the selectron propagators $D_{(t,u)(L,R)}$ in Eq. (7). Moreover, the optimal variables would depend on both selectron masses. For simplicity, we construct our CP–odd observables by fully including the angular dependence in the *numerators* of Eqs. (17), (18), (21), (22), (23) and (29), but ignoring the angular dependence in the propagators.

For dimensionless f, the quantity F in Eq. (30) is also dimensionless. The statistical uncertainty of F is then given by

$$\sigma^2(F) = \mathcal{L} \times \int d\Omega \frac{d\sigma}{d\Omega} f^2(\Omega)\,. \tag{32}$$

This can be seen from the fact that $\mathcal{L}(d\sigma/d\Omega)d\Omega$ is the number of events in the phase space interval $d\Omega$. For the simple case of $f = \pm 1$, $\sigma^2(F)$ is simply the total number of events. With the quantity F and its statistical uncertainty $\sigma(F)$, we can construct an effective asymmetry:

$$\hat{A}[f] = \frac{F}{\sigma(F)\sqrt{\mathcal{L}}}\,. \tag{33}$$

Note that $\hat{A}$ is by construction independent of the luminosity. It is also invariant under transformations $f(\Omega) \to c f(\Omega)$ for constant c, making $\hat{A}$ independent of the normalization of f. The statistical significance for $\hat{A}[f]$ is simply given by $\hat{A}[f] \cdot \sqrt{\mathcal{L}}$.

6 Numerical analysis

We are now ready to present some numerical results. We will first briefly discuss the relevant quartic charges that encode CP violation, before discussing "production" and "decay" asymmetries.

6.1 Quartic charges

Table 1 shows that the four quartic charges Q_4, Q_6, Q_4' and Q_6' are CP-odd. Equation (18) shows that Q_6' is responsible for the production–level asymmetry, which requires transverse beam polarization.* The remaining three CP–odd quartic charges can be probed only via the $\tilde{\chi}_2^0$ polarization. Equations (22) and (23) show that Q_4 contributes even for unpolarized $e^{\pm}$ beams, whereas Q_4' (Q_6) only contributes in the presence of longitudinal (transverse) beam polarization.

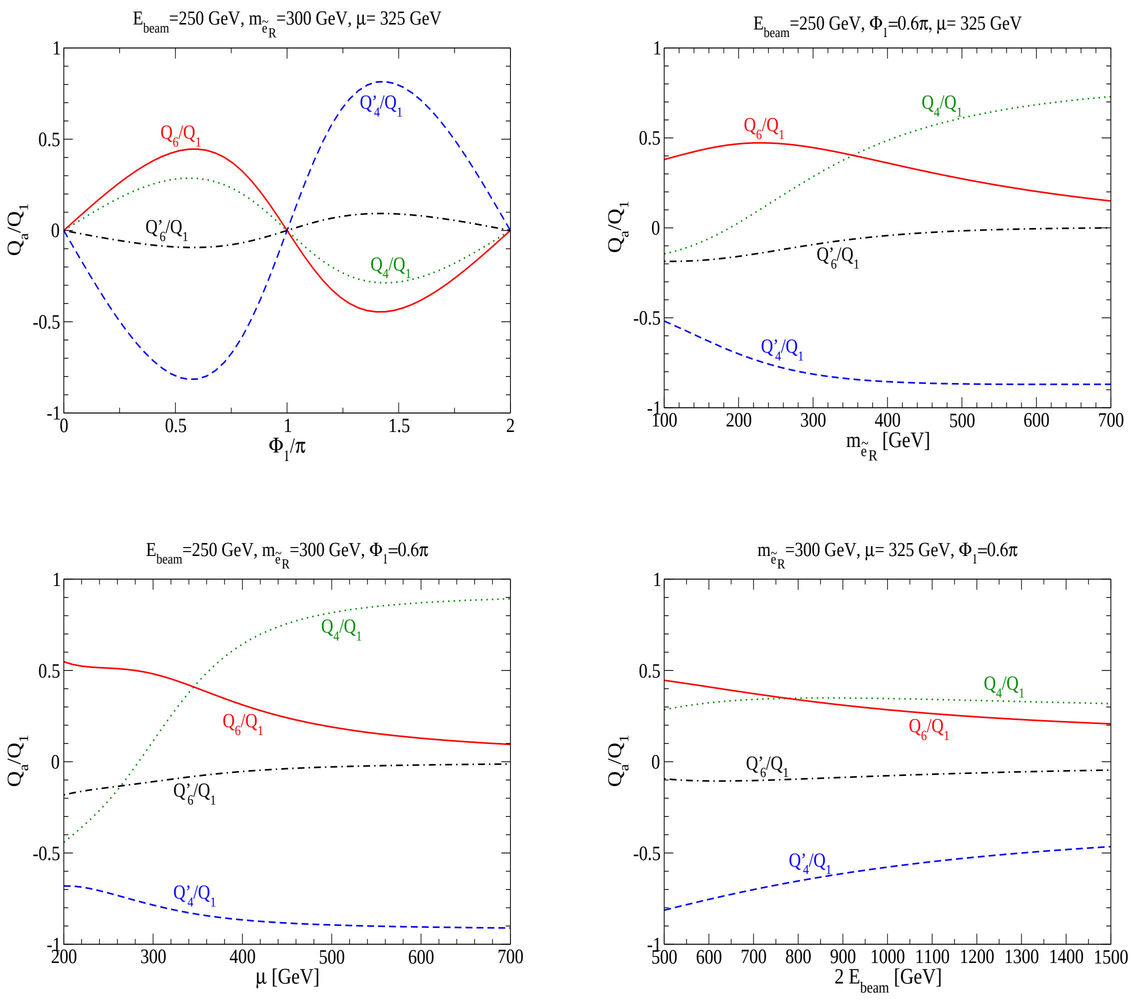

Figure 2: *The ratios of quartic charges Q_4/Q_1 (dotted green), Q_4'/Q_1 (dashed blue), Q_6/Q_1 (solid red) and Q_6'/Q_1 (dot–dashed black). We fixed $|M_1| = 0.5 M_2 = 150$ GeV, $\tan\beta = 5$, $m_{\tilde{e}_L} = 500$ GeV and $\Phi_\mu = 0$; the values of the other relevant parameters are as indicated in the figures.*

Figure 2 presents these four charges normalized to Q_1, which largely determines the size of the unpolarized cross section far above threshold. All these ratios lie between -1

*We note in passing that the corresponding asymmetry for chargino production vanishes [17]: there is no equivalent of the $\tilde{e}_R$ exchange diagram, and the relevant 2×2 matrix diagonalizing the chargino mass matrix does not contain a reparametrization invariant phase.

and 1. We took $|M_1| = 150$ GeV, $M_2 = 300$ GeV (so that $|M_1|$ and M_2 unify at the scale of Grand Unification [1]), a moderate $\tan\beta = 5$, $m_{\tilde{e}_L} = 500$ GeV, and $\Phi_\mu = 0$ (as indicated by constraints on the electric dipole moments of the electron and neutron [2, 3]). The default choices of the other relevant parameters are $|\mu| = 325$ GeV, $m_{\tilde{e}_R} = 300$ GeV, $\Phi_1 = 0.6\pi$ and $\sqrt{s} = 2E_{\rm beam} = 500$ GeV, but one of these parameters is varied in each of the four frames of Fig. 2. Finally, we chose scattering angle $\cos\Theta = 1/\sqrt{2}$; note that Q'_6 vanishes at $\cos\Theta = 0$.

The behavior of the curves in Fig. 2 can be understood with the help of the expressions in Eq. (26). The top–left frame shows the dependence of the four ratios on the phase Φ_1. We see the typical behavior of CP–odd quantities, changing sign when $\sin\Phi_1$ changes sign, although not simple sine functions. Since we took $|\mu|$ to be close to M_2, $\tilde{\chi}^0_2$ is a strongly mixed state. However, $\tilde{\chi}^0_1$ is still mostly gaugino–like, so that $|\mathcal{Z}_{12}|$ is quite small. As a result, increasing $m_{\tilde{e}_R}$ (top–right frame) reduces $|Q_6|$ and $|Q'_6|$, while affecting $|Q_4|$ and $|Q'_4|$ very little; recall that the latter two quartic charges receive the dominant contribution from the interference of $t-$ and $u-$channel $\tilde{e}_L$ exchange diagrams. Increasing $|\mu|$ (bottom–left frame) has the same effect, as expected from our earlier observation that Q_6 and Q'_6 need sizable gaugino–higgsino mixing, while Q_4 and Q'_4 do not. Finally, the bottom–right frame shows that the dependence on the beam energy is relatively mild.

Another conclusion from Fig. 2 is that $|Q'_6|$ is usually the smallest of the four CP–odd quartic charges. The reason is that in this case $t-$ and $u-$channel diagrams tend to cancel, whereas they add up in $|Q_6|$. This indicates that measuring the production–level asymmetry will be quite challenging, as will be discussed in the next Subsection.

6.2 Production asymmetries

The simplest choice for probing the CP–odd contribution from Q'_6 to the production cross section in Eq. (17) is [8]

$$f_{\rm prod} = {\rm sign}[\cos\Theta\sin(2\Phi)]\,. \tag{34}$$

Instead a partly optimized asymmetry is suggested from the choice

$$f^{\rm opt}_{\rm prod} = \cos\Theta\sin^2\Theta\sin(2\Phi)\,, \tag{35}$$

where we have set the angle $\eta = 0$ for simplicity; nothing is gained by considering non-vanishing angles between the transverse e^+ and e^- polarization vectors. The factors of $\sin^2\Theta$ and $\sin(2\Phi)$ appear explicitly in the differential cross section in Eq. (17); inclusion of the factor $\cos\Theta$, which strictly speaking violates the construction principle described in Sec. 5, is necessary in this case, since this contribution to the cross section changes sign when $\cos\Theta \to -\cos\Theta$.

Here it is appropriate to show that the asymmetries defined in Eqs. (30), (34) and (35) are indeed CP–odd. This can most easily be seen by using the so–called naive or $\widetilde{\rm T}$ transformation, which inverts the signs of all three–momenta and spins, but (unlike a true T–transformation) does not exchange initial and final state. In the absence of absorptive phases[†] a violation of $\widetilde{\mathrm{T}}$ invariance is equivalent to CP violation, as long as CPT is conserved (which is certainly the case in the MSSM). Recall that we fixed the $+z$ and $+x$ directions via the e^- beam and spin directions, respectively, which are themselves $\widetilde{\mathrm{T}}$ odd quantities.[‡] In this coordinate frame a $\widetilde{\mathrm{T}}$ transformation therefore amounts to flipping the signs of only the $y-$components of all three–momenta and spins. This is equivalent to flipping the sign of the azimuthal angle Φ (as well as that of Φ^*, which is however irrelevant for the production–level asymmetry), leaving Θ (and Θ^*) unchanged. Our production–level asymmetries are therefore $\widetilde{\mathrm{T}}$ odd, which probe CP–violation if absorptive phases can be ignored.

The effective asymmetries resulting from Eqs. (34) and (35) are shown by the (green) dotted and (black) solid curves, respectively, in three frames in Fig. 3. In these figures we have chosen the same default parameters as in Fig. 2, which ensures that $\tilde{\chi}_2^0 \to \tilde{\chi}_1^0 Z$ is the only possible two–body decay of $\tilde{\chi}_2^0$.[§] As noted in Sec. 3, in this case we can measure the $\tilde{\chi}_2^0$ polarization only if the polarization of the Z boson is determined. In particular, one has to be able to distinguish between the two transverse polarization states in order to construct CP–odd asymmetries involving the Z polarization. Although this measurement is, in principle, possible for $Z \to \ell^+\ell^-$ decays, the efficiency is quite low due to its small branching ratio ($\sim 7\%$ after summing over e and μ final states), and a very poor analyzing power (from almost purely axial vector coupling for $Z\ell^+\ell^-$). Although $q\bar{q}$ final states have larger analyzing power, the measurement of the charge is very difficult. It may be only possible to probe the production level asymmetry through this decay mode.

Unfortunately the event cannot be reconstructed in this mode, as noted in Sec. 4. This means that we do not know the angles Θ and Φ appearing in the definitions of Eqs. (34) and (35); the best we can do is to approximate them by the corresponding angles of the Z boson. This leads to the (blue) dashed curves in the frames of Fig. 3 that show effective asymmetries, which are based on the "optimized" choice in Eq. (35).

The top–left frame shows these asymmetries as functions of the CP–odd phase Φ_1. We see that the "optimized" effective asymmetry exceeds the simple asymmetry based on Eq. (34) by typically $\sim 20\%$, leading to a $\sim 40\%$ reduction of the luminosity required to establish the existence of a non–vanishing asymmetry at a given confidence level. Unfortunately replacing the true production angles (Θ and Φ) by those of the Z boson reduces the effective asymmetry by a factor of 2.5$-$3.5. This suppression factor depends on the masses of the two lightest neutralinos, which in turn depend on Φ_1. In this case even for the most favorable choice of parameters an integrated luminosity of several ab^{-1} would be needed to establish a non–vanishing optimized asymmetry at the 1σ level, even assuming 100% beam polarization! This is well beyond the currently expected performance of the international linear collider.

[†]In the present context absorptive phases can only come from the finite width in the $Z-$propagator, which is entirely negligible for $s \gg m_Z^2$, or from loop corrections.

[‡]Note that for $\eta = 0$ the initial state is $\widetilde{\mathrm{T}}$ self–conjugate in this coordinate frame.

[§]The effective asymmetry constructed from $\tilde{\chi}_2^0 \to \tilde{\chi}_1^0 h$ decays is very similar to that from $\tilde{\chi}_2^0 \to \tilde{\chi}_1^0 Z$ decays; we therefore do not show numerical results for this decay mode.

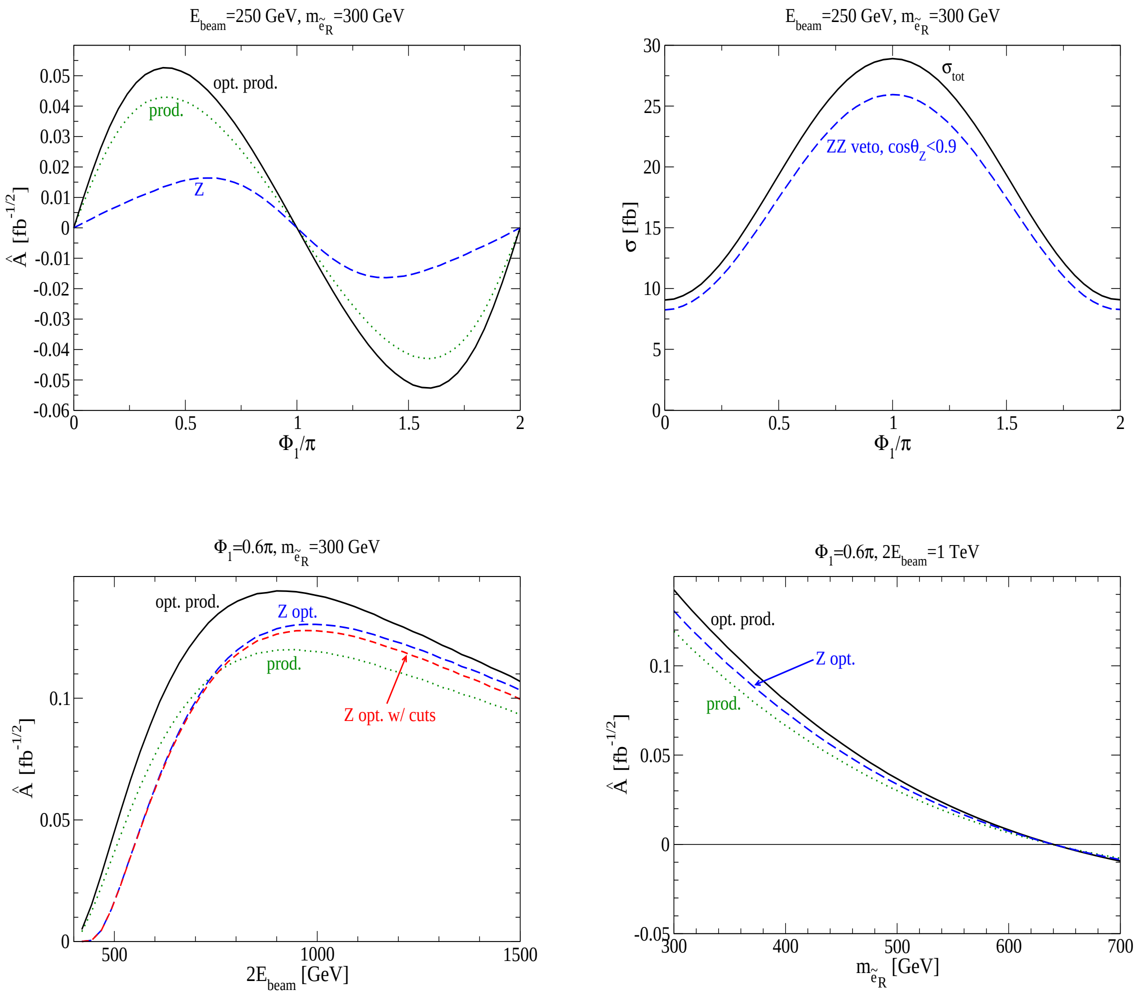

Figure 3: *The top–left and both bottom frames show the effective production–level asymmetries defined by Eq. (34) (green dotted curves, labeled "prod.") and (35) (solid black curves, labeled "opt. prod."), together with the "optimized" production asymmetry where the true production angles are replaced by those reconstructed from the Z direction (blue long–dashed curves: without cuts; red short–dashed curve: with the cuts described in the text). The top–right frame shows the total cross section for $e^+e^- \to \tilde{\chi}_1^0\tilde{\chi}_2^0$ without (black solid curve) and with (blue dashed curve) cuts. The default parameters are as in Fig. 2, but one parameter is varied in each frame.*

The lower–left frame of Fig. 3 shows that the situation might be better at higher beam energies. The effective production asymmetries peak at $\sqrt{s} \simeq 900$ GeV for the given choice of SUSY parameters. Moreover, the difference between the "theoretical" optimized asymmetry and the one constructed from the Z boson angles becomes much smaller at higher energy. The reason is that at $\sqrt{s} \gg m_{\tilde{\chi}_2^0}$ the $\tilde{\chi}_2^0$ becomes ultra–relativistic; its decay products then fall in a narrow cone around the $\tilde{\chi}_2^0$ direction, so that the differences between the real production angles (Θ and Φ) and the corresponding angles derived from the flight direction of the Z boson become small. However, even in this case 1 ab^{-1} would only allow to establish an asymmetry with a significance of 3.5 standard deviations at best, ignoring experimental resolutions and efficiencies, and assuming 100% transverse beam polarization. The bottom–right frame shows that the situation is even worse if the mass of the SU(2) singlet selectron $\tilde{e}_R$ is close to that of the SU(2) doublet $\tilde{e}_L$, which is taken as 500 GeV in this figure.

The top–right figure is a reminder that $\tilde{\chi}_1^0\tilde{\chi}_2^0$ production can nevertheless provide useful information on the phase Φ_1 [4], simply through a measurement of the total production cross section, which increases by almost a factor of three when Φ_1 is varied from 0 to π; no beam polarization is needed for this measurement. As explained in Refs. [11, 4] this is due to the fact that the production occurs in a pure $P-$wave for $\Phi_1 = 0$, but has a large $S-$wave component for $\Phi_1 = \pi$. This figure also shows that, for the chosen set of parameters, cutting against the ZZ background as described in Sec. 4, as well as applying the acceptance cut

$$|\cos\Theta_X| \leq 0.9 \tag{36}$$

for all visible final state particles X (in this case, the Z boson), only reduces the cross section by $\sim 15\%$. The (red) short–dashed curve in the bottom–left frame shows that these cuts affect the effective asymmetries even less.

6.3 Decay asymmetries

We now turn to the "decay" asymmetries, which are sensitive to the $\tilde{\chi}_2^0$ polarization. We saw in Sec. 3 that these can be only probed through $\tilde{\chi}_2^0 \to \tilde{\ell}^\pm\ell^\mp$ decays (ignoring three–body decays, which will be highly suppressed if any two–body decay is allowed). The discussion of Sec. 4 showed that in this case we can reconstruct the event with two– or four–fold ambiguity.

Equation (21) shows that there are three CP–odd terms in the $\tilde{\chi}_2^0$ polarization vector, which are sensitive to transverse beam polarization. In order to construct the corresponding "optimized" asymmetries, we first need an explicit expression for the scalar product appearing in Eq. (29). Working in the reference frame where the $+x$ direction is defined by the transverse part of the e^- polarization vector, and using the same set of axes for the definition of the $\tilde{\chi}_2^0$ decay angles Θ^*, Φ^* in the $\tilde{\chi}_2^0$ rest frame, we find using Eqs. (24) and (25):

$$\begin{aligned} \overrightarrow{\mathcal{P}} \cdot \hat{k}_1^* \;=\; & \mathcal{P}_T \left[\cos\Theta\sin\Theta^*\cos(\Phi-\Phi^*) - \sin\Theta\sin\Theta^*\right] \\ & + \mathcal{P}_L \left[\sin\Theta\sin\Theta^*\cos(\Phi-\Phi^*) + \cos\Theta\cos\Theta^*\right] \\ & + \mathcal{P}_N \sin\Theta^*\sin(\Phi-\Phi^*)\,, \end{aligned} \tag{37}$$

where we have suppressed the superscript 2 on the components of the $\tilde{\chi}_2^0$ polarization vector. This, together with Eqs. (21) and (23), leads to the following choices for f in

Eq. (30):*

$$
\begin{aligned}
f_{LN} &= [\sin\Theta\sin\Theta^*\cos(\Phi-\Phi^*)+\cos\Theta\cos\Theta^*]\sin(2\Phi)\sin^2\Theta\,,\\
f_{TN} &= [\cos\Theta\sin\Theta^*\cos(\Phi-\Phi^*)-\sin\Theta\sin\Theta^*]\sin(2\Phi)\sin(2\Theta)\,,\\
f_{NT} &= [\sin\Theta^*\sin(\Phi-\Phi^*)]\cos(2\Phi)\sin\Theta\,.
\end{aligned} \tag{38}
$$

In each of the three expressions the factor in square brackets comes from Eq. (37), the second factor from Eq. (21), and the last factor from the expressions for Σ_{LN}, Σ_{TN} and Σ_{NT}, respectively, in Eq. (23).

Similarly, the expression for Δ_N^{21} in Eq. (21) contains two CP–odd terms that can be probed with only longitudinal beam polarization, or even with unpolarized beams. Since the expressions for Σ_{NU} and Σ_{NL} in Eqs. (22) and (23) are identical except for different quartic charges, we can combine these two terms into the "optimized" longitudinal effective asymmetry $\hat{A}_L \equiv \hat{A}[f_L]$ with

$$
f_L = [\sin\Theta^*\sin(\Phi-\Phi^*)]\sin\Theta\,. \tag{39}
$$

Note that the four functions f_i defined in Eqs. (38) and (39) are all orthogonal to each other, i.e., the product of any two different functions will vanish when integrated over the entire phase space.

Although the three asymmetries defined in Eqs. (38) are independent of each other (probing different Σ_{AB}), in the context of the MSSM they all probe the same quartic charge Q_6. If $m_{\tilde{\chi}_1^0}$ and $m_{\tilde{\chi}_2^0}$ are known, one can therefore construct a single asymmetry to probe Q_6, called the total "optimized" transverse decay asymmetry $\hat{A}_T \equiv \hat{A}[f_T]$ with

$$
\begin{aligned}
f_T &= [\sin\Theta\sin\Theta^*\cos(\Phi-\Phi^*)+\cos\Theta\cos\Theta^*]\sin(2\Phi)\sin^2\Theta\cdot\left(1+\mu_1^2-\mu_2^2\right)\\
&+ [\cos\Theta\sin\Theta^*\cos(\Phi-\Phi^*)-\sin\Theta\sin\Theta^*]\sin(2\Phi)\sin(2\Theta)\cdot\mu_2\\
&+ [\sin\Theta^*\sin(\Phi-\Phi^*)]\cos(2\Phi)\sin\Theta\cdot 2\mu_2\,,
\end{aligned} \tag{40}
$$

where the μ_i have been defined in Eq. (5). The first, second and third line in Eq. (40) correspond to the contributions from Σ_{LN}, Σ_{TN} and Σ_{NT}, respectively.

Finally, we also consider an effective asymmetry based on the measurement of the momentum of the positive lepton ℓ_1 coming from the first stage of $\tilde{\chi}_2^0$ decay, defined by $\hat{A}_1^+ \equiv \hat{A}[f_1^+]$ with

$$
f_1^+ = \sin(2\Phi_{\ell_1^+})\,. \tag{41}
$$

The advantage of this asymmetry, which is somewhat similar to the decay asymmetry considered in Ref. [8], is that it does not need event reconstruction, as long as the "primary" and "secondary" leptons can be distinguished.

As discussed in the previous Subsection, a CP–odd observable changes sign when $\Phi \to -\Phi$ and $\Phi^* \to -\Phi^*$. Evidently the asymmetries defined in Eqs. (38) through (41)

*Note that the denominator Δ_U^{21} in Eq. (20) cancels against the factor Δ_U^{21} from the production cross section (17) in the final result for the cross section differential in production and decay angles.

satisfy this condition. Due to the sign flip in Eq. (29) all asymmetries discussed in this Subsection have opposite signs for $\tilde{\chi}_2^0 \to \tilde{\ell}_R^+ \ell^-$ and $\tilde{\chi}_2^0 \to \tilde{\ell}_R^- \ell^+$ decays; events of these two kinds should be treated separately. Since there are equal number of events from these two decay chains, we can simply focus on events with only positively charged primary leptons.

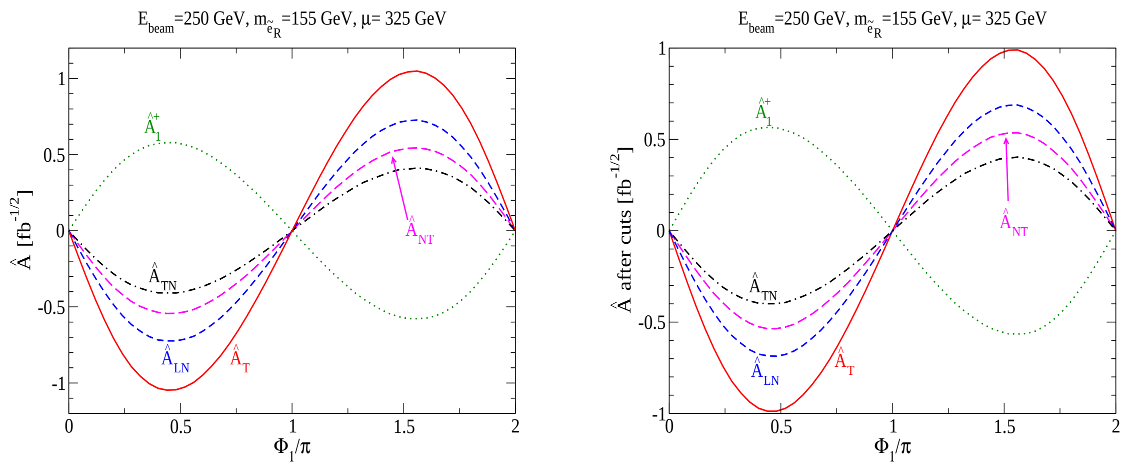

Figure 4: *Effective transverse decay asymmetries for the same default parameters as in Fig. 2, except that now $m_{\tilde{e}_R} = 155$ GeV. The (black) dot–dashed, (magenta) long dashed and (blue) short dashed curves show the "optimized" asymmetries based on f_{TN}, f_{NT} and f_{LN} in Eq. (38), respectively, while the (red) solid curves show $\hat{A}_T$ of Eq. (40), and the (green) dotted curves show $\hat{A}_1^+$ of Eq. (41). In the right (left) frame acceptance and background–removing cuts have (not) been applied.*

The two figures in Fig. 4 show the effective "optimized" decay asymmetries based on Eqs. (38), (40) and (41). We use the same default parameters as in Figs. 2 and 3, except that the $\tilde{e}_R$ mass has been reduced to 155 GeV, so that $\tilde{\chi}_2^0 \to \tilde{e}_R^\pm e^\mp$ decays are allowed and dominant. Our choice of $m_{\tilde{e}_R}$ implies that $m_{\tilde{\chi}_2^0} - m_{\tilde{e}_R} \gg m_{\tilde{e}_R} - m_{\tilde{\chi}_1^0}$. As discussed in Sec. 4 this implies that the harder lepton always comes from the first step of $\tilde{\chi}_2^0$ decay, allowing to reconstruct the event with only a two–fold ambiguity. We average over both of these solutions when calculating the "optimized" asymmetries. We find that the wrong reconstruction typically leads to asymmetries with the same sign as the true solution, with (of course) smaller magnitude. The dilution of the asymmetries due to the event reconstruction ambiguity is therefore not very severe. The effective asymmetry based on f_{LN} of Eq. (38) and, especially, the one based on f_T of Eq. (40) are therefore substantially larger in magnitude than the simple effective asymmetry based on Eq. (41). Note also that the three effective asymmetries based on Eq. (38) move "in step", as expected from our earlier observation that they all probe the same quartic charge Q_6. Combining them into a single effective asymmetry, as in Eq. (40), therefore increases the size of the asymmetry significantly.

The two frames in Fig. 4 differ in that the left figure does not include any cuts whereas in the right figure we remove events that can be reconstructed as W or $\tilde{e}_R$ pair background events. Also, we apply the acceptance cut in Eq. (36) to both final state leptons. For the case at hand these cuts only reduce the effective asymmetries by 10% to 20%. This high cut efficiency is also due to our choice of masses, which implies that the two leptons in the final state have very different energies. In contrast, both background processes have identical energy distributions for the two leptons in the final state. Signal events can be rarely reconstructed as background in this scenario. As a result we find that even after cuts one would only need an integrated luminosity of ~ 10 fb^{-1} to measure a non–vanishing asymmetry at the 3σ level. This still assumes 100% beam polarization. Even for the more realistic choice $P_T \overline{P}_T \simeq 0.5$ one might achieve 3σ significance with ~ 40 fb^{-1} of data. This integrated luminosity should be achievable, assuming that transverse beams will be available.

Finally, the four figures in Fig. 5 compare the simple asymmetry $\hat{A}_1^+$ of Eq. (41), the total optimized transverse decay asymmetry $\hat{A}_T$, and the optimized longitudinal decay asymmetry $\hat{A}_L$. We note that the *longitudinal* decay asymmetry is usually *bigger* than our total optimized *transverse* asymmetry. At least for probing the CP-violating phase in the context of the MSSM (where Φ_1 is the only relevant phase in the convention where M_2 is real), therefore, one does not really seem to gain anything by transverse beam polarization. The only exception is at large energy (bottom–right frame); this is due to the extra factor $m_{\tilde{\chi}_1^0}/\sqrt{s}$ appearing in the expressions for Σ_{NU} in Eq. (22), and Σ_{NL} in Eq. (23), which determine the size of $\hat{A}_L$.

The upper right panel shows a quite complicated dependence of the effective asymmetries on $m_{\tilde{e}_R}$. For intermediate $\tilde{e}_R$ masses both final–state leptons in signal events can have similar energies. As a result one often has four solutions for the event reconstruction. In this case one cannot identify the "primary" lepton used in Eq. (41). We have dealt with this by simply discarding events with four solutions, since averaging over all four solutions would dilute the asymmetries a lot. Unfortunately this reduces the cross section significantly. At the same time $\tilde{e}_R$ pair events become more similar to our $\tilde{\chi}_1^0\tilde{\chi}_2^0$ events, since, as we just mentioned, the signal now has similar distributions for both final $\ell^\pm$ energies. Hence the cut against selectron pair production removes more signal events in the present case. As a result, the complete set of cuts reduces the total cross section by up to a factor of 5, the worst case being $m_{\tilde{e}_R} \simeq 195$ GeV. Note that the different asymmetries are not equally sensitive to these cuts. The total "optimized" transverse decay asymmetry $\hat{A}_T$ is reduced by at worst a factor of 2, whereas the simple asymmetry $\hat{A}_1^+$ can go down by a factor of 4. The reason for this is that the cut efficiency depends on the same production and decay angles that appear in the definitions of our asymmetries.

The lower left panel includes the longitudinal decay asymmetry $\hat{A}_L$ for two different choices of longitudinal $e^\pm$ beam polarization. In both cases we take opposite polarization for the e^+ and e^- beams, since we are dealing with chiral couplings, see Eq.(11). Usually taking a right–handed electron beam is most advantageous, since it maximizes the $\tilde{e}_R$ exchange contribution; note that the $\tilde{e}_R$ coupling to Binos, which is needed to probe the CP–odd phase Φ_1, is two times larger than that of $\tilde{e}_L$. However, for very large $|\mu|$ this

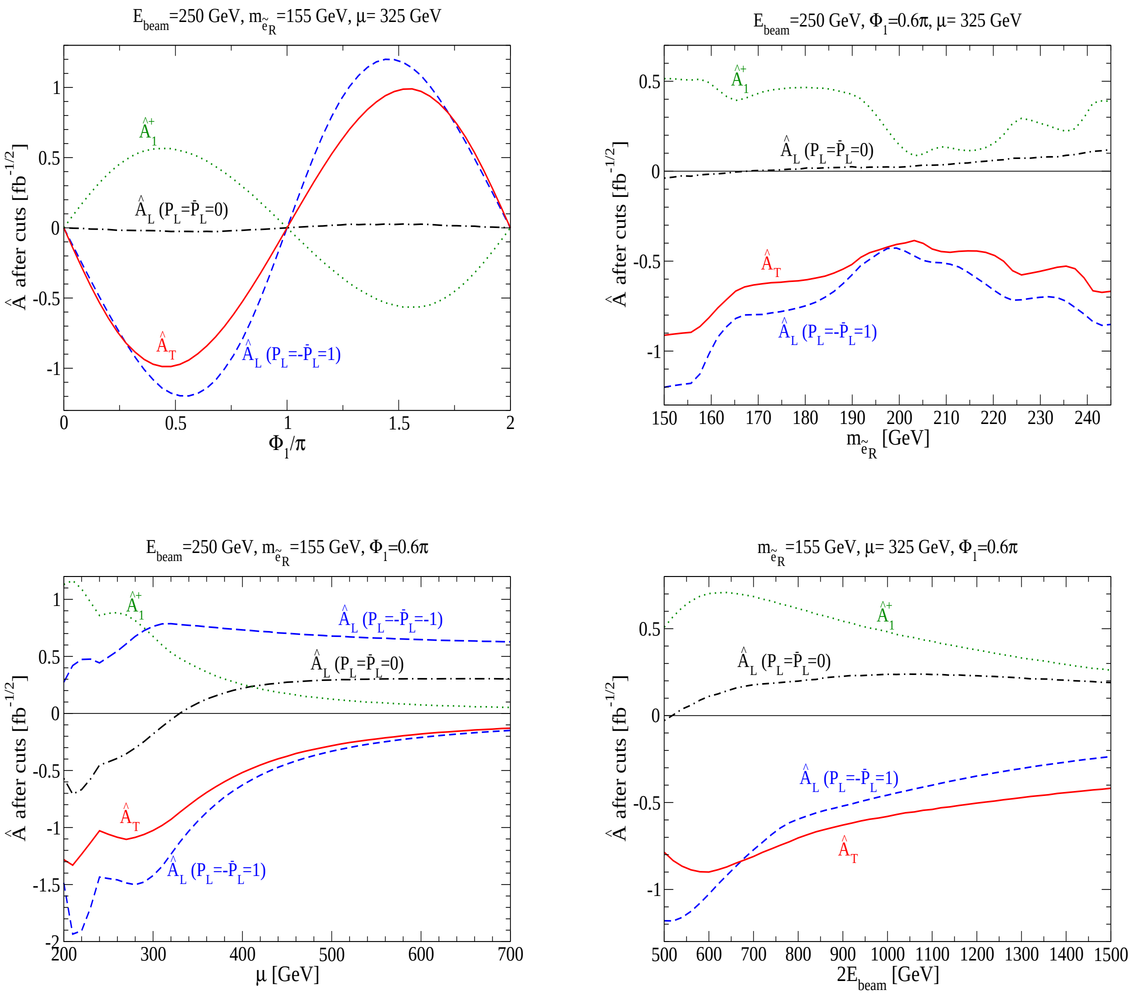

Figure 5: *Comparison of the simple transverse decay asymmetry (41) (green dotted curves), the total "optimized" transverse decay asymmetry (40) (red solid curves), and the "optimized" longitudinal decay asymmetry (39), the latter both for transverse (black dot–dashed) and for longitudinal (blue dashed) beam polarization. The default values of the parameters are as in Fig. 4, but one parameter is varied in each panel.*

choice is no longer optimal. In this case $\tilde{\chi}_2^0$ becomes more and more wino–like, i.e., it does not couple to $\tilde{e}_R$. A right–handed e^- beam means that $\tilde{e}_L$ exchange does not contribute; the Z–exchange contribution also vanishes for large $|\mu|$. However, taking left–handed electrons one still gets a sizable contribution from $\tilde{e}_L$ exchange to the cross section, and also to the asymmetry. In the opposite regime of rather small $|\mu|$ the asymmetries depend very strongly on this parameter, since here $\tilde{\chi}_2^0$ changes from a higgsino-like to a wino–like state.

As in the previous figures (as well as in Ref. [8]) we took $e^\pm$ beam polarizations ± 1.

In the case of longitudinal beams one can then suppress the W or $\tilde{e}_R$ pair background (but not both), by appropriate choice of polarization. However, in practice the beam polarization will be significantly smaller than this; we therefore left the cuts against both backgrounds in place. We also note that longitudinal beam polarization can increase $\hat{A}_L$ significantly, although the very small size of this effective asymmetry for our "default" parameters and transversely polarized beams (top left frame) is clearly accidental.

Last but not least, we have checked numerically the effect of varying the left–handed selectron mass $m_{\tilde{e}_L}$ on the CP–odd asymmetries. The transverse decay asymmetries, with transversely polarized beams, are sensitive to the mass; in fact, they get a bit bigger with smaller mass values. Nevertheless, we have noted that the longitudinal asymmetry for unpolarized beams becomes much bigger when the left–handed selectron mass is reduced. For example, taking parameters as in the top–left frame in Fig. 5, except for a reduced $m_{\tilde{e}_L} = 250$ GeV, the maximal value of $|\hat{A}_T|$ after cuts increases to about 1.2 fb$^{-1/2}$, whereas the maximum of $|\hat{A}_L|$ reaches about 2.2 fb$^{-1/2}$. We emphasize that we do not actually need any beam polarization to probe this asymmetry, although it can be increased significantly by using longitudinal polarized beams; for reduced $\tilde{e}_L$ mass, taking left–handed e^- and right–handed e^+ beams is often optimal. Therefore, reducing the left–handed selectron mass does not affect the ordering of A_T and A_L, i.e. the inequality $A_L > A_T$ (for optimized choice of longitudinal beam polarization.)

7 Summary and Conclusions

In this paper we studied the production of neutralino pairs at future linear e^+e^- colliders, with subsequent two–body decays of the heavier neutralinos. We found that decays of the type $\tilde{\chi}_i^0 \to \tilde{\chi}_j^0(h, Z)$ are not sensitive to the $\tilde{\chi}_i^0$ polarization, unless one can measure the polarization of the $Z-$boson (or that of the final–state neutralino $\tilde{\chi}_j^0$). These decays can therefore only be used to probe CP violation in neutralino *production*. Unfortunately the corresponding CP–odd term suffers from cancelations between $t-$ and $u-$channel diagrams, and is nonzero only in the presence of higgsino–gaugino mixing. As a result, measuring this asymmetry, which can be done only with transversely polarized $e^\pm$ beams, will be very difficult, if not impossible, with the currently foreseen linear collider performance.

In contrast, $\tilde{\chi}_i^0$ decays into a slepton plus a lepton allows to probe the $\tilde{\chi}_i^0$ polarization state, thereby opening up the possibility to construct several decay asymmetries. Moreover, this decay, followed by subsequent $\tilde{\ell} \to \ell\tilde{\chi}_1^0$ decays, allows to reconstruct even the simplest neutralino pair events, $\tilde{\chi}_2^0\tilde{\chi}_1^0$ production with invisible (e.g., stable) $\tilde{\chi}_1^0$, with two– or four–fold ambiguity. Under favorable circumstances experiments at a collider with (sufficiently strongly) transversely polarized beams should then be able to determine non–vanishing asymmetries with high statistical significance. However, even in this case a different asymmetry, which does not depend on transverse beam polarization (but can be maximized using longitudinal beam polarization), is generally larger in size than even the best of the transverse decay asymmetries we studied. We saw in Fig. 5 that this is true both for gaugino– and higgsino–like $\tilde{\chi}_2^0$. It also remains true when we vary the ratio $|M_1|/M_2$, in particular for $|M_1| > M_2$. However, if $|M_1| \gg M_2$, $|\mu|$, or if both produced neutralinos are higgsino–like, all CP–odd asymmetries become small. Recall that in the MSSM all these asymmetries essentially result from a single (potentially large) phase, associated with the U(1) gaugino mass (in the convention where the SU(2) gaugino mass is real and positive).

We therefore conclude that, *at least* in the context of neutralino production in the MSSM, transverse beam polarization is not particularly useful in probing explicit CP violation. Once the relevant masses have been determined, the most sensitive probe of the relevant CP–odd phases remains the total cross section [4], although it is a CP–even observable. If this measurement indicates that some phase differs from 0 or π, one needs to see explicit CP violation, in order to convince oneself that the variation of the cross section is indeed due to a phase, rather than due to some extension of the MSSM. However, as noted above, this can be most easily accomplished by using longitudinal, rather than transverse, beam polarization.

The situation might be different in extensions of the MSSM, however. Whenever the quartic charges Q_6 and Q_6' defined in Sec. 2.2 contain (combinations of) phases that are independent of those in Q_4 and Q_4', the option of transverse beam polarization might be very useful for determining these phases. In the NMSSM, for example, the neutralino mass matrix contains additional CP–odd phases associated with the singlino sector, which can be large. A dedicated analysis along the lines presented in this paper would be required to decide whether transverse beam polarization could be helpful in disentangling this more complicated neutralino sector.

Acknowledgments

We thank Saurabh Rindani for discussions that triggered this investigation, and Peter Zerwas for discussions and suggestions. The work of JS was supported by the Korea Research Foundation Grant (KRF-2005-070-C00030). The work of SYC was supported partially by the Korea Research Foundation Grant (KRF–2004–041–C00081) and by KOSEF through CHEP at Kyungpook National University. MD thanks the Center for Theoretical Physics at Seoul National University, as well as the particle theory group at the University of Hawaii at Manoa, for hospitality.

References

[1] M. Drees, R.M. Godbole and P. Roy, *Theory and Phenomenology of Sparticles*, World Scientific (Singapore, 2004); D.J.H. Chung, L.L. Everett, G.L. Kane, S.F. King, J. Lykken and L.T. Wang, Phys. Rep. **407**, 1 (2005).

[2] J.R. Ellis, S. Ferrara and D.V. Nanopoulos, Phys. Lett. B **114**, 231 (1982); F. del Aguila, M.B. Gavela, J.A. Grifols and A. Mendez, Phys. Lett. B **126**, 71 (1983), Erratum-ibid. B **129**, 473 (1983).

[3] T. Ibrahim and P. Nath, Phys. Lett. B **418**, 98 (1998); Phys. Rev. D **57**, 478 (1998); D **58**, 019901 (1998) (E); *ibid*, 111301 (1998); *ibid.* D **61**, 095008 (2000), hep–ph/9907555; M. Brhlik, G.J. Good and G.L. Kane, Phys. Rev. D **59**, 115004 (1999), hep–ph/9810457; M. Brhlik, L.L. Everett, G.L. Kane and J.D. Lykken, Phys. Rev. Lett. **83**, 2124 (1999), hep–ph/9905215.

[4] S.Y. Choi, M. Drees and B. Gaissmaier, Phys. Rev. D **70**, 014010 (2004), hep–ph/0403054.

[5] S.T. Petcov, Phys. Lett. B **178**, 57 (1986); Y. Kizukuri and N. Oshimo, Phys. Lett. B **249** (1990) 449; V. Barger, T. Han, T. Li and T. Plehn, Phys. Lett. B **475**, 342 (2000), hep–ph/9907425; V.D. Barger, T. Falk, T. Han, J. Jiang, T. Li and T. Plehn, Phys. Rev. D **64**, 056007 (2001), hep–ph/0101106; J. Kalinowski, Acta Phys. Polon. B **34**, 3441 (2003), hep–ph/0306272; A. Bartl, H. Fraas, O. Kittel and W. Majerotto, Phys. Rev. D **69**, 035007 (2004), hep–ph/0308141, and Eur. Phys. J. C **36**, 233 (2004), hep–ph/0402016; A. Bartl, H. Fraas, S. Hesselbach, K. Hohenwarter–Sodek and G. Moortgat–Pick, JHEP **0408**, 038 (2004), hep–ph/0406190; S.Y. Choi, Phys. Rev. D **69**, 096003 (2004), hep–ph/0308060.

[6] S.Y. Choi, H.S. Song and W.Y. Song, Phys. Rev. D **61**, 075004 (2000), hep–ph/9907474.

[7] A. Bartl, T. Kernreiter and O. Kittel, Phys. Lett. B **578**, 341 (2004), hep–ph/0309340; S.Y. Choi, M. Drees, B. Gaissmaier and J. Song, Phys. Rev. **D69**, 035008 (2004), hep–ph/0310284.

[8] A. Bartl, H. Fraas, S. Hesselbach, K. Hohenwarter-Sodek, T. Kernreiter and G. Moortgat-Pick, hep–ph/0510029.

[9] J.R. Ellis, J.M. Frère, J.S. Hagelin, G.L. Kane and S.T. Petcov, Phys. Lett. B **132**, 436 (1983); V. Barger, R.W. Robinett, W.Y. Keung and R.J.N. Phillips, Phys. Lett. B **131**, 372 (1983); A. Bartl, H. Fraas and W. Majerotto, Nucl. Phys. B **278**, 1 (1986), and Z. Phys. C **30**, 441 (1986); G. Moortgat–Pick and H. Fraas, Phys. Rev. D **59**, 015016 (1999), hep–ph/9708481]; G. Moortgat–Pick, H. Fraas, A. Bartl and W. Majerotto, Eur. Phys. J. C **9**, 521 (1999), Erratum-ibid. C **9**, 549 (1999), hep–ph/9903220; G. Moortgat-Pick, A. Bartl, H. Fraas and W. Majerotto, Eur. Phys. J. C **18**, 379 (2000), hep–ph/0007222.

[10] T. Tsukamoto, K. Fujii, H. Murayama, M. Yamaguchi and Y. Okada, Phys. Rev. D **51**, 3153 (1995); J.L. Feng, M.E. Peskin, H. Murayama and X. Tata, Phys. Rev. D **52**, 1418 (1995), hep–ph/9502260: H. Baer, R. Munroe and X. Tata, Phys. Rev. D **54**, 6735 (1996), Erratum-ibid. D **56**, 4424 (1997), hep–ph/9606325; J.L. Kneur and

G. Moultaka, Phys. Rev. D **59**, 015005 (1999), hep–ph/9807336, and Phys. Rev. D **61**, 095003 (2000), hep–ph/9907360; G.A. Blair, W. Porod and P.M. Zerwas, Phys. Rev. **D63**, 017703 (2001), hep–ph/0007107.

[11] S.Y. Choi, J. Kalinowski, G. Moortgat-Pick and P.M. Zerwas, Eur. Phys. J. C **22**, 563 (2001); *ibid.* C **23**, 769 (2002).

[12] D. Pierce and A. Papadopoulos, Phys. Rev. D **50**, 565 (1994), hep–ph/9312248, and Nucl. Phys. B **430**, 278 (1994), hep–ph/9403240; A.B. Lahanas, K. Tamvakis and N.D. Tracas, Phys. Lett. B **324**, 387 (1994), hep–ph/9312251; H. Eberl, M. Kincel, W. Majerotto and Y. Yamada, Phys. Rev. D **64**, 115013 (2001), hep–ph/0104109; T. Fritzsche and W. Hollik, Eur. Phys. J. C **24**, 619 (2002), hep–ph/0203159; W. Oller, H. Eberl, W. Majerotto and C. Weber, Eur. Phys. J. C **29**, 563 (2003), hep–ph/0304006; W. Oller, H. Eberl and W. Majerotto, Phys. Lett. B **590**, 273 (2004), hep–ph/0402134.

[13] K. Hagiwara and D. Zeppenfeld, Nucl. Phys. B **274**, 1 (1986); G.A. Ladinsky, Phys. Rev. D **46**, 2922 (1992).

[14] J.F. Gunion and H.E. Haber, Phys. Rev. D **37**, 2515 (1988); S.Y. Choi and Y.G. Kim, Phys. Rev. D **69**, 015011 (2004).

[15] A. Djouadi, M. Drees and J.-L. Kneur, JHEP **0108**, 055 (2001), hep–ph/0107316.

[16] D. Atwood and A. Soni, Phys. Rev. D **45**, 2405 (1992); M. Diehl and O. Nachtmann, Z. Phys. C **62**, 397 (1994); M. Davier, L. Duflot, F. Le Dieberder and A. Rougé, Phys. Lett. B **306**, 411 (1993); J.F. Gunion, B. Grzadkowski and X.-G. He, Phys. Rev. Lett. **77**, 5172 (1996).

[17] A. Bartl, K. Hohenwarter–Sodek, T. Kernreiter and H. Rud, Eur. Phys. J. C **36**, 515 (2004), hep–ph/0403265.